Int J Adv Manuf Technol (2017) 90:2557–2565
DOI 10.1007/s00170-016-9582-4

ORIGINAL ARTICLE

The influence of the cutting tool microgeometry on the machinability of hardened AISI 4140 steel

Carlos E. H. Ventura[1] · **Heitor S. Chaves**[2] · **Juan Carlos Campos Rubio**[3] · **Alexandre M. Abrão**[3] · **Berend Denkena**[4] · **Bernd Breidenstein**[4]

Received: 5 July 2016 / Accepted: 7 October 2016 / Published online: 19 October 2016

Abstract The performance of cutting tools can be drastically affected by cutting edge preparation i.e. the presence of a radius and/or a chamfer and their dimensions can alter cutting forces and temperature and, consequently, tool life as well as the surface quality of the machined component. The aim of this work is to investigate the machinability of AISI 4140 steel hardened to 40 HRC and 50 HRC when turning with coated tungsten carbide inserts with various microgeometries (brushed edges with distinct slopes). The following aspects were considered: cutting force components, cutting temperature and machined surface roughness. In comparison with the published literature, the novelty of the present work is related to the investigation of the machinability of a hardened steel by applying a large variety of customized non-commercial cutting edge geometries. Differently from other studies, the paper presents experimental results for temperature in the contact zone employing different cutting edge geometries. Moreover, in order to explain the results, an analysis of tool-workpiece contact zone is carried out for each edge geometry. The results indicated that cutting edge microgeometry affects mainly the feed and passive force components, while the cutting force, specific energy and cutting temperature are not drastically altered. Finally, no clear relationship between microgeometry and machined surface roughness was noticed, although irregular marks on the roughness profile were found when sharp edges were used (suggesting edge chipping) and evidence of side flow was noted when rounded edges were tested.

Keywords Turning · Hardened AISI 4140 steel · Cutting edge preparation · Cutting force · Cutting temperature · Surface roughness

✉ Alexandre M. Abrão
abrao@ufmg.br

[1] Department of Mechanical Engineering, Federal University of São Carlos, Rodovia Washington Luís km 235, São Carlos, SP 13565-905, Brazil

[2] Faculty of Mechanical Engineering, State University of Campinas, Caixa Postal 6122, Campinas, SP 13083-860, Brazil

[3] Department of Mechanical Engineering, Universidade Federal de Minas Gerais, Avenida Antônio Carlos 6627, Belo Horizonte, MG 31270-901, Brazil

[4] Institute of Production Engineering and Machine Tools, Leibniz Universität Hannover, An der Universität 2, 30823 Garbsen, Germany

1 Introduction

Although hardness, toughness and chemical affinity with the work material are critical aspects to be considered when selecting the most appropriate cutting tool for a given operation, the influence of cutting edge geometry cannot be disregarded, irrespectively of the work material properties and operation severity. For instance, in spite of their low hardness, the elevated ductility of aluminium alloys demands the usage of cutting tools with a highly positive rake angle. In contrast, a negative rake angle is crucial for the successful machining of grey cast irons due to their fragile nature. Furthermore, changes in tool geometry can drastically act upon cutting forces and temperature, which in turn will restrict tool life and the quality of the machined component, thus affecting production costs. However, for a given cutting edge geometry, substantial improvements on the outputs of the operation can be obtained by changing its microgeometry i.e. its cutting edge preparation. More specifically, the association of proper microgeometry with micro-grained tungsten carbide has allowed the application of this tool grade to turning of

steels with moderately high hardness, area previously dominated by polycrystalline cubic boron nitride (PcBN) and alumina-based ceramics.

Since de advent of PcBN tooling in the 1970s, the machinability of hardened steels has been extensively investigated aiming at replace cylindrical grinding and although the tightest dimensional and geometric tolerances attainable by grinding have not been obtained using single point cutting tools, substantial benefits have been achieved concerning the surface integrity of turned hardened steels. Benlahmidi et al. [1] investigated the influence of the cutting parameters on the machinability of hardened AISI H11 steel (40–50 HRC) subjected to turning with PcBN tools and noticed that surface roughness (R_t parameter) decreases with the elevation of cutting speed and workpiece hardness and increases with the reduction of feed rate, while the influence of depth of cut was considered negligible. Tang et al. [2] reported that increasing workpiece hardness from 51 to 62 HRC leads to the elevation of the process forces; however, a further increase to 65 HRC results in the reduction of the forces, probably caused by the increase in brittleness and consequent reduction of the tensile strength of the work material.

In general, hard turning is accomplished employing round or chamfered cutting edges (or their combination) which are used; nevertheless, they can be generated through distinct operations such as grinding, brushing and blasting and with particular features governing their performance. An alternative technique for edge preparation is presented by Yussefian et al. [3], who used electrical discharge machining to generate distinct edge hones and chamfers with the aid of an especially designed counterface. The results showed narrower scatter in the dimensions of the edges and longer tool lives in comparison with conventionally prepared cutting edges when facing annealed AISI 1045 steel with high speed steel tools. A low cost laser marking equipment was used by Aurich et al. [4] to generate edge radii ranging from 9 to 47 μm on uncoated cemented carbide tools applied to face milling of cast iron, and the findings indicated that longer tool lives and better machined surface roughness were obtained by the laser rounded edges in comparison with a commercial product. Additionally, the performance of the prepared tools improved with the dimension of the generated hone radius. Two distinct approaches for edge honing of tungsten carbide inserts used for turning of austenitic stainless steel were tested by Fernández-Abia et al. [5]: blasting of glass microspheres and drag-grinding, in which the inserts describe a planetary motion inside an abrasive medium. The inserts were further coated and the tests indicated that drag-grinding promoted lower process forces and machined surface roughness together with a more uniform tool wear.

Laser-textured patterns were produced on the rake face of tungsten carbide inserts used for turning of AISI 4340 steel hardened to 55 HRC [6]. In order to reduce friction, the cavities were filled with a solid lubricant (CaF_2) prior to the turning tests and the influence of five texture parameters (distance from the cutting edge, area width, pitch, diameter and depth of the cavities) on process forces was investigated. The findings indicated that pitch distance presented the most significant influence on process forces; however, significant interaction was observed between distance from the edge, area width and pitch distance.

In their classic work, Thiele and Melkote [7] investigated hard turning of a bearing steel using PcBN tooling with distinct microgeometries: commercially available (nominal radius of 25.4 μm), intermediate honed edges (radii ranging from to 76.2 to 127 μm), large honed edges (101.6–152.4 μm) and chamfered edges (114.3 μm × 17°). The findings indicated that statistically significant changes in the cutting force were observed for extreme values of edge hones (the larger the radius, the higher the cutting force), while the thrust force (resultant of the passive and feed forces) increased with edge radius. Edge preparation was found to be more influential on the thrust force than feed rate and as far as the surface roughness (R_a parameter) is concerned, its value increased with hone radius, although the influence of the latter decreased with the elevation of workpiece hardness. The influence of the cutting edge radius (ranging from 100 to 1200 μm) on tool wear and process forces when turning a case-hardened steel with PcBN tools was carried out by Meyer et al. [8], who noticed that the flank wear rate decreased with the elevation of edge radius, presenting little variation for edge radii above 400 μm. In contrast, the passive force increased remarkably with edge radius followed by the cutting force, while the feed force was much less affected.

Chinchanikar and Choudhury [9] proposed a model to predict the process force evolution with tool wear when hard turning AISI 4340 steel (35 and 45 HRC) with coated tungsten carbide inserts and found that a satisfactory agreement between the experimental and modelled values was obtained for gradual flank wear values below 0.2 mm; however, the difference between both approaches increased as tool wear progressed, probably owing to the influence of cutting edge chipping.

A comparison between the performances of chamfered (0.1 mm × 25°) and honed (r_β = 20 μm) PcBN tools in orthogonal cutting of hardened hot work die steel was carried out by Özel [10], who noted that higher process forces were recorded when cutting with the chamfered tool due to the decrease in the effective rake angle. In contrast, finite element simulations indicated that higher temperatures in the tool-chip interface were found using the honed tool. Similarly, Denkena et al. [11] studied the effect of edge honing (based on the cutting edge segments on the flank and rake faces, S_α and S_γ, respectively) on the normalized resultant force F'_z (N/mm) and temperature near the cutting edge of cemented tungsten carbide tools in orthogonal cutting of AISI 1045

medium carbon steel. The results showed that neither the normalized resultant force nor the cutting edge temperature were affected by changes in the value of S_γ, whereas the elevation of S_α led to higher normalized resultant force. Kurt and Seker [12] investigated the influence of the chamfer angle on the cutting and passive forces in hard turning of a bearing steel using PcBN tools and noted that both the cutting and passive force components were elevated when the chamfer angle increased from 0° to 30°. Moreover, the passive force was more affected than the cutting force.

As far as the effect of edge geometry on tool wear is concerned, Chen et al. [13] compared the tool lives of honed and chamfered PcBN tools when turning a hardened tool steel and noticed that longer tool life was obtained employing the latter microgeometry. Moreover, while abrasion was the principal wear mechanism observed on chamfered tools, the life of honed tools was limited by abrasion at lower feed rate and by catastrophic failure at higher feed rate. Interestingly, higher temperatures were numerically estimated at the cutting edge when the chamfered tool was used, probably due to the larger workpiece stagnation zone (chip speed close to zero), which could act as a protective layer and prevent tool wear. Similar results concerned with the life of mixed alumina tools in hard turning of a tool steel were reported by Davoudinejad and Noordin [14], who also noticed that lower surface roughness was obtained using a chamfered tool, although the honed insert provided a more steady roughness behaviour with the evolution of tool wear.

Finite element modelling was employed by Khalili and Safaei [15] to simulate orthogonal cutting of a low alloy steel using chamfered cemented carbide tools. The presence of a stagnation zone in the cutting edge was identified; however, a larger degree of straining was noted in the lower region of the flank face not protected by the stagnation zone, which could lead to accelerated flank wear rates. Similar work was carried out by Denkena et al. [16], though focused on honed tools. The findings suggested that the size of the stagnation zone increased with edge radius and was larger for symmetrically rounded than for asymmetrically rounded edges. Furthermore, in the latter case, the influence of S_α (cutting edge segment on the flank face) was much larger than the influence of S_γ (cutting edge segment on the rake face), considered negligible. Consequently, the feed force increased significantly with S_α and was not affected by S_γ and the location of the maximum cutting temperature shifted to either the flank face or to the rake face with the respective increase in S_α or S_γ.

Denkena and Biermann [17] report that investigations concerned with the influence of cutting edge preparation have received considerable attention over the last years, with a dramatic increase in the number of published papers since 2002. Nevertheless, the authors state that several questions regarding the integrity of the tool and cutting performance remain unanswered. Within this scenario, this work offers a more comprehensive approach in which the relationships between cutting force components, cutting temperature and machined surface finish are addressed when turning AISI 4140 steel with two levels of hardness and employing micro-grained tungsten carbide inserts with a wide range of microgeometries.

2 Experimental procedure

Bars of AISI 4140 low alloy high strength steel (diameter of 75 mm and length of 300 mm) were quenched and tempered to reach two levels of hardness: 40 ± 1 HRC and 50 ± 1 HRC. Tungsten carbide inserts ISO grade H20 and geometry SNMN 120408 were used as cutting tools and the selected microgeometries were produced through brushing with a KUKA KR16 industrial robot using 240 mesh SiC brushes. After brushing, the inserts received a TiAlN coating layer by physical vapour deposition. As material removal during brushing corresponds to a force-linked operation, the

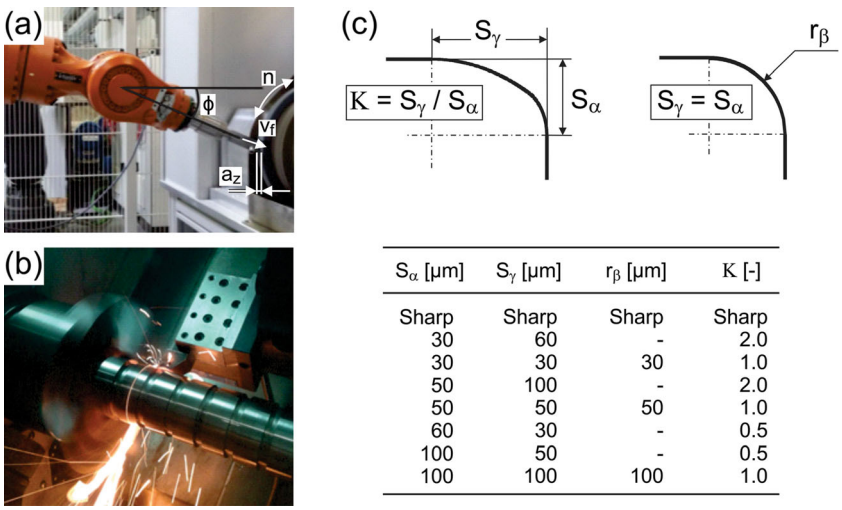

S_α [μm]	S_γ [μm]	r_β [μm]	K [-]
Sharp	Sharp	Sharp	Sharp
30	60	-	2.0
30	30	30	1.0
50	100	-	2.0
50	50	50	1.0
60	30	-	0.5
100	50	-	0.5
100	100	100	1.0

Fig. 1 **a** Brushing setup, **b** experimental setup for cutting forces measurement and **c** microgeometry parameters and selected S_α and S_γ values

Table 1 Brushing parameters

S_γ [μm]	S_α [μm]	First step				Second step			
		n [rpm]	a_z [mm]	v_f [mm/s]	ϕ [°]	n [rpm]	a_z [mm]	v_f [mm/s]	ϕ [°]
60	30	2100	0.5	1.0	60	−1200	0.2	5.0	45
30	30	2000	0.5	1.0	47	−1200	0.2	1.0	42
50	50	2000	0.6	1.2	55	−1500	0.5	1.2	35
30	60	1950	0.5	1.0	50	−1750	0.5	1.0	30
100	50	2400	0.5	0.2	60	−1300	0.2	2.0	45
100	100	2300	0.5	0.4	60	−1950	0.5	0.7	35
50	100	2200	0.3	0.9	50	−2200	0.3	0.6	30

following parameters (Fig. 1a) should be set through an iterative process in order to achieve the correct edge geometry: brush rotation (n), penetration depth (a_z), feed speed (v_f) and inclination angle (ϕ). Each insert edge was prepared by two steps: material removal with positive brush rotation direction (brushing at the rake face–adjustment of S_γ) and material removal with negative brush rotation direction (brushing at the flank face–adjustment of S_α). The applied parameters are shown in Table 1.

Continuous dry turning tests were performed on a CNC lathe at constant cutting speed and depth of cut (90 m/min and 0.5 mm, respectively) and using two levels of feed rate (0.15 and 0.30 mm/rev). During the trials, the three components of the resultant force were measured with a Kistler piezoelectric dynamometer model 9121 connected to a National Instruments acquisition board model BNC 2110. The temperature of the chip at the rake face was measured with a Raytec Marathon MM2ML infrared pyrometer (emissivity adjusted to 0.76 at a temperature of 300 °C). Finally, average roughness (R_a) of the machined surface was measured with a Taylor Hobson Form Talysurf 50 roughness metre set to a cut-off of 0.80 mm. Measurements of process forces, cutting temperature and surface roughness were carried out along a workpiece length of 20 mm. Fresh cutting tools were always used in order to avoid the influence of tool wear on the investigated outputs. Two replicates were conducted for each cutting condition and the average value was used to plot the graphs.Figure 1a shows the experimental setup for brushing, Fig. 1b shows the experimental setup for cutting forces measurement and Fig. 1c presents the microgeometry parameters as well as the selected S_α and S_γ values.

3 Results and discussion

The values for S_α and S_γ before and after coating (assessed using a GFM MikroCAD scanner) are presented in Fig. 2a, b, respectively, where it can be noted that accuracy decreases and scatter increases after coating and with the elevation of S_α and S_γ. Furthermore, it can be seen that the cutting edges

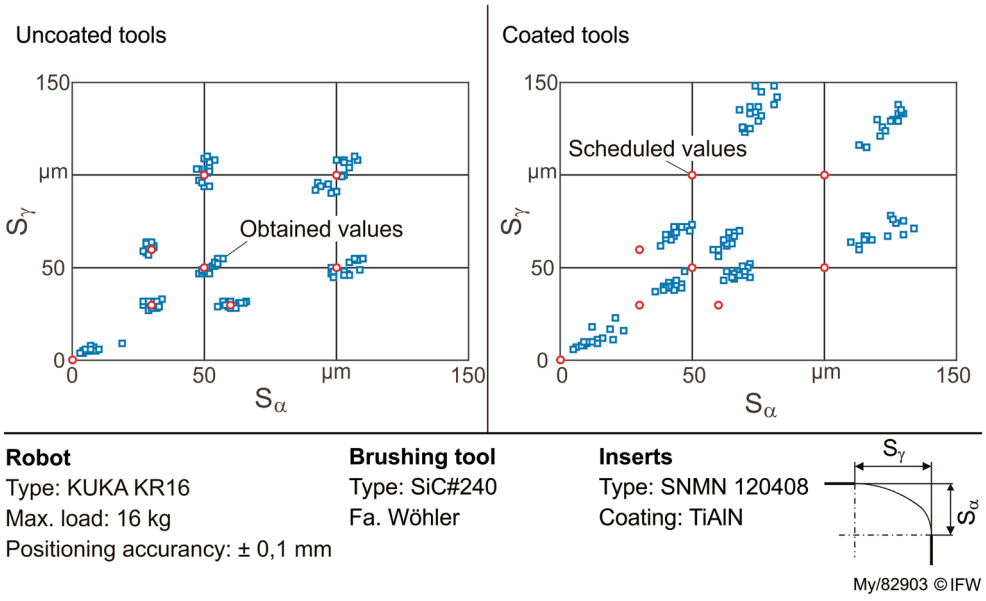

Fig. 2 Actual values for S_α and S_γ after brushing and coating

Table 2 Experimental results

	$S_\gamma \times S_\alpha$ [μm × μm]	F_p [N]	F_f [N]	F_c [N]	F_{thr}/F_c [–]	e [J/mm^3]	T [°C]	R_a [μm]
	Sharp	205.8	144.0	325.3	0.8	4337.1	535.0	–
	60 × 30	282.6	188.8	349.9	1.0	4665.1	572.5	–
	30 × 30	245.3	163.8	345.7	0.9	4609.2	608.2	–
40 HRC	100 × 50	309.0	196.6	337.5	1.1	4499.7	523.0	–
f = 0.15 mm	50 × 50	314.0	188.9	351.2	1.0	4682.7	579.8	–
	30 × 60	322.8	188.8	351.4	1.1	4684.7	639.0	–
	50 × 100	578.2	283.0	400.1	1.6	5334.5	567.5	–
	100 × 100	508.2	264.5	383.4	1.5	5112.1	546.3	–
	Sharp	257.7	152.0	466.2	0.6	3108.3	474.5	4.0
	60 × 30	315.8	171.7	445.1	0.8	2967.4	484.6	4.9
	30 × 30	266.0	150.2	436.4	0.7	2909.6	480.2	5.3
40 HRC	100 × 50	414.1	221.5	510.0	0.9	3400.0	456.6	4.6
f = 0.30 mm	50 × 50	349.4	177.1	449.2	0.9	2994.9	502.4	5.0
	30 × 60	436.9	202.1	487.0	1.0	3246.9	442.9	4.2
	50 × 100	518.6	222.4	489.2	1.2	3261.3	455.0	4.6
	100 × 100	633.8	281.2	561.2	1.2	3741.0	486.9	5.4
	Sharp	262.2	172.2	393.1	0.8	5241.5	585.0	–
	60 × 30	480.1	330.3	424.3	1.4	5656.9	612.5	–
	30 × 30	444.1	245.4	385.6	1.3	5141.1	615.0	–
50 HRC	100 × 50	617.8	319.6	341.1	2.0	4547.7	618.8	–
f = 0.15 mm	50 × 50	703.5	355.4	401.6	2.0	5354.7	632.5	–
	30 × 60	812.8	401.1	408.5	2.2	5446.7	669.5	–
	50 × 100	1415.9	614.1	459.2	3.4	6123.2	570.0	–
	100 × 100	1063.8	455.4	392.2	3.0	5229.1	605.0	–
	Sharp	492.7	244.8	495.6	1.1	3303.8	535.0	3.3
	60 × 30	531.1	267.4	468.6	1.3	3123.7	572.5	4.8
	30 × 30	512.9	241.1	459.4	1.2	3062.5	608.2	3.9
50 HRC	100 × 50	704.7	261.6	428.7	1.8	2858.2	523.0	4.9
f = 0.30 mm	50 × 50	672.6	307.3	474.2	1.6	3161.6	579.8	5.0
	30 × 60	843.8	328.3	463.0	2.0	3086.5	639.0	4.1
	50 × 100	967.9	285.3	389.5	2.6	2596.3	567.5	4.5
	100 × 100	1114.0	373.1	466.0	2.5	3106.7	546.3	5.7

F_p passive force, F_f feed force, F_c cutting force, F_{thr} thrust force, e specific energy, T temperature, R_a average surface roughness

considered sharp possess average S_α and S_γ values of, respectively, 13.1 and 11.6 μm. Table 2 summarizes the experimental results obtained after the turning tests.

Figure 3 shows the force components obtained when turning employing different edge geometries at two levels of feed rate and workpiece hardness. Irrespectively of the microgeometry, the increment in feed rate for both workpieces has mainly affected the cutting force (F_c) with an increase of approximately 25 % due to the larger shear area. This increase is not proportional to the feed rate elevation due to a nonlinear decrease in the specific cutting force typically observed when feed rate is elevated. Considering the greater difficulty in shearing the work material by all kinds of edge geometries, an increase in workpiece hardness leads to an increase in the passive (F_p) and feed (F_f) forces. In general, the passive force increased nearly 100 %, while the feed force presented an increase of approximately 50 %. The cutting force remained approximately constant as workpiece hardness was elevated.

In hard turning, cutting edge rounding is typically applied in order to reinforce the cutting edge and increase tool life by avoiding edge chipping. This should lead to a more stable process and gradual tool wear. However, a decrease in sharpness due to cutting edge preparation causes higher chip deformation and, consequently, higher process forces. Moreover, in comparison with sharp edges, rounded edges can increase tool-workpiece contact length and the friction between tool

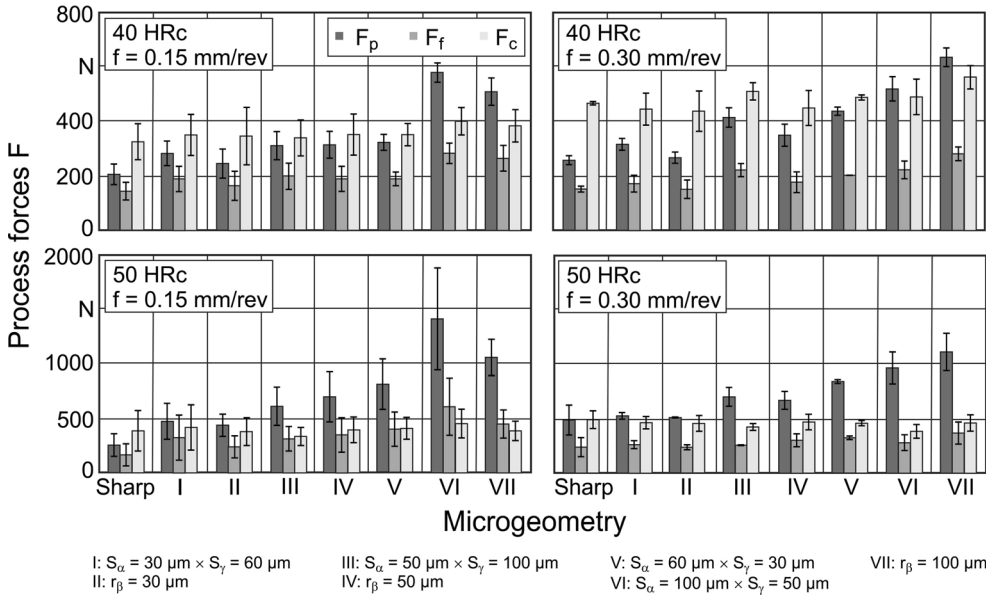

Fig. 3 Resultant force components measured for different edge geometries, feed rates and workpiece hardness values

and workpiece. Though edge preparation enhances edge stability, such side effects can impair the operation. From the left to the right side of Fig. 3, there is a reduction in edge sharpness with a consequent increase of tool-workpiece contact length l_k (observed from the normal plane, see Fig. 4). The bluntness of the edge makes it harder to penetrate the workpiece material, causing an increase of both passive and feed forces, which are more sensitive to changes in microgeometry than the cutting force. Due to the fact that tool nose radius (r_ε = 0.8 mm) is larger than depth of cut (a_p = 0.5 mm), the uncut chip thickness decreases towards the tool tip and most of the chip is formed at the rounded edge at highly negative rake angles; thus, ploughing becomes dominant. Since the force related to this phenomenon is projected on the plane perpendicular to cutting direction, the passive and feed force components are more affected. Similar results were observed by Meyer et al. [8], who tested different edge radii, and Kurt and Seker [12], who varied the angle of chamfered edges.

Higher forces are mainly obtained by employing higher values of S_α due to a more dramatic increase in the contact length compared to higher S_γ values. These findings agree with the results reported by Denkena et al. [11], Denkena et al. [16] and Basset et al. [18].

The growth rate of the cutting force is not as significant as that observed for the passive and feed forces, as the former is mainly related to shearing of the work material. Thus, the effect of microgeometry on the forces can be better observed by the analysis of the ratio between the resultant force on the tool reference plane (thrust force) and the cutting force. High thrust forces can impair workpiece dimensional tolerances and therefore must be avoided. An increase in this ratio for blunter tools can be observed in Fig. 5a. Considering both feed rates,

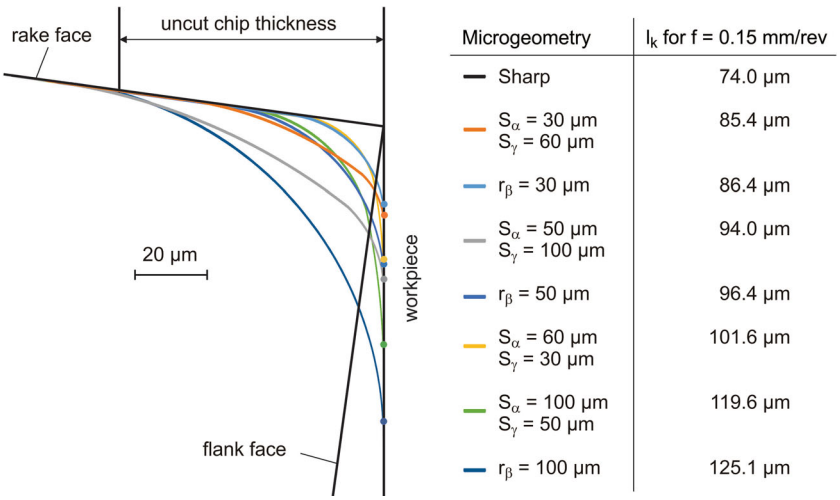

Fig. 4 Tool-workpiece engagement considering different edge geometries

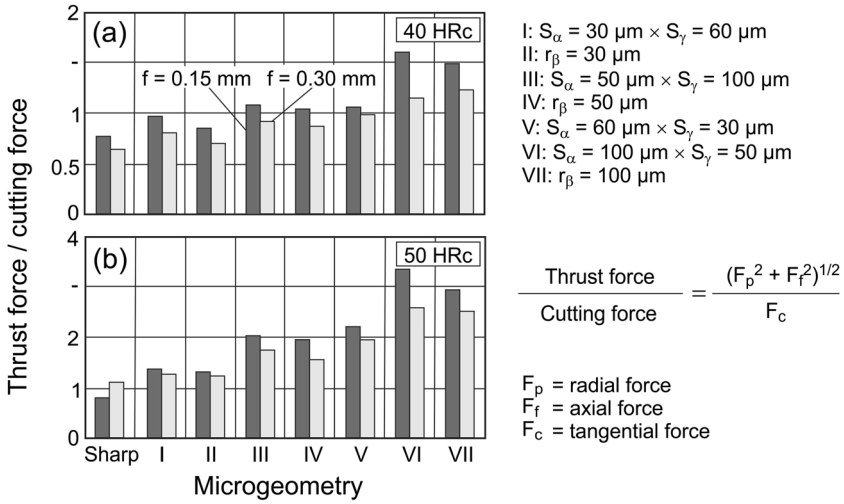

Fig. 5 Ratio between thrust and cutting force for different edge geometries and feed rates: **a** workpiece hardness of 40 HRC and **b** workpiece hardness of 50 HRC

thrust force is higher for the last two microgeometries (S_α = 100 μm × S_γ = 50 μm and r_β = 100 μm). By increasing workpiece hardness, however, cutting force is equal or higher than the thrust force (thrust force/cutting force ≤1) only for the sharp tool (Fig. 5b) due to the higher material strength. An increase in feed rate corresponds to an increase in the uncut chip thickness and, therefore, leads to a reduction of the ratio between thrust and cutting forces.

Regarding cutting efficiency, specific energy was not altered by microgeometry, see Fig. 6a. As changes in cutting force with microgeometry are not significant, the uncut chip thickness does not depend on it and the thrust force does not affect cutting power; therefore, energy consumption is not changed by microgeometry. However, increasing workpiece hardness leads to a slightly higher specific energy, while the increase in feed rate reduces the specific energy by 25 %, thus elevating cutting efficiency. These results can be compared with Fig. 6b, which shows that chip temperature is also approximately constant for the different edge geometries tested and increases slightly with workpiece hardness. As most of the mechanical energy is converted into thermal energy during cutting, the specific energy can be directly related to heat generation. Therefore, the evolution of temperature should comply with the general behaviour of specific energy, as previously depicted. Discussions focused on cutting efficiency were not found in the literature, though some authors [10, 13] observed distinct cutting temperatures by simulating the application of different edge geometries through finite element methods. Nevertheless, there is no agreement among the reported results.

The effect of microgeometry on the machined surface average roughness (R_a) can be observed in Fig. 7a. For both workpiece hardness values, surface roughness presents approximately the same level ($R_a \cong$ 4–5 μm), and a clear relationship with edge geometry is not observed. In contrast, Thiele and Melkote [7] reported that an increase of edge radius leads to higher values of surface roughness; however, these authors noted that the influence of edge radius decreased at

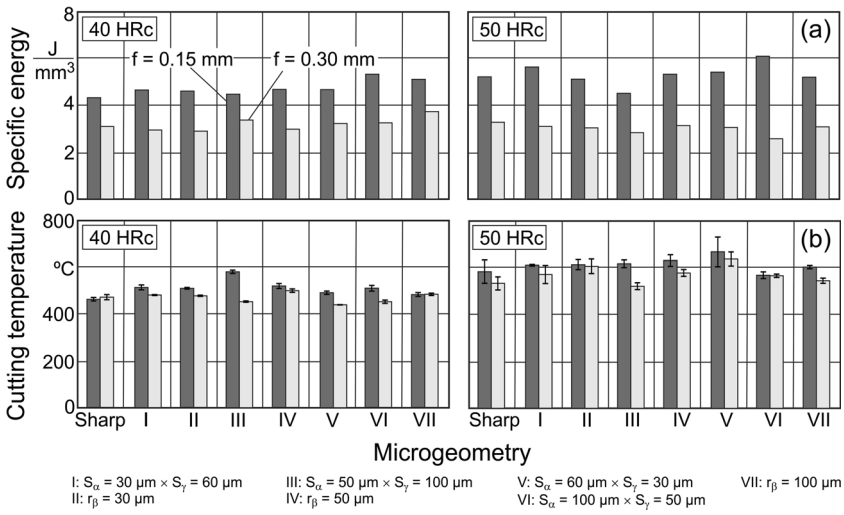

Fig. 6 **a** Specific energy and **b** chip temperature for different edge geometries, feed rates and workpiece hardness values

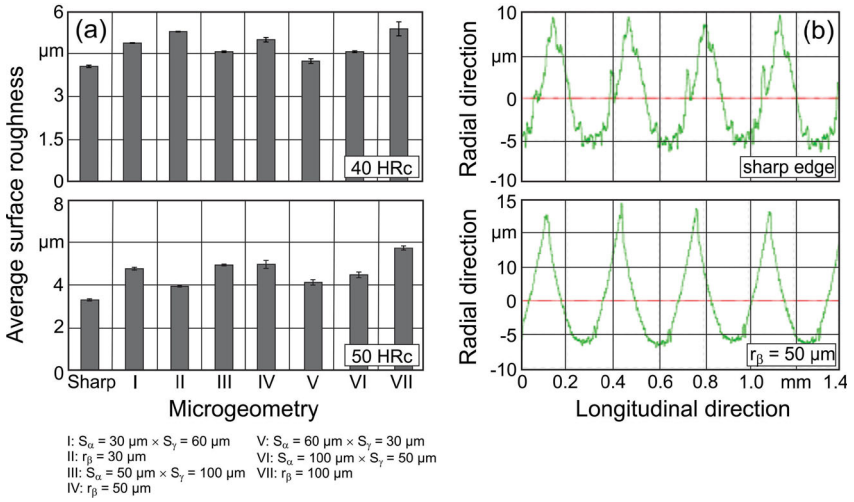

Fig. 7 **a** Effect of microgeometry and workpiece hardness on average surface roughness (f = 0.3 mm/rev). **b** Roughness profile generated by a sharp and an edge prepared with r_β = 50 μm (workpiece hardness of 40 HRC, f = 0.3 mm/rev)

higher workpiece hardness values, thus supporting the presented results.

The usage of a sharp edge leads to the lowest roughness values, while an edge preparation possessing r_β = 100 μm leads to the highest R_a values. This is associated, respectively, with the smallest and largest material deformations during chip formation, demonstrated by the cutting force components. A non-smooth roughness profile was generated by the sharp edge when compared to the profiles obtained using rounded edges (Fig. 7b), since higher edge chipping of the sharp tool is responsible for leaving irregular marks on the machined surface. Similar marks are also observed in the valleys of the roughness profile generated by honed cutting edges, but these can be attributed to the reduced chip thickness in that region, which causes high material deformation and consequent side flow, thus impairing workpiece surface, especially in the case of the material with lower hardness (more ductile).

4 Conclusion

After conducting continuous dry turning tests on AISI 4140 steel with two levels of hardness (40 HRC and 50 HRC) using PVD-coated tungsten carbide tools with seven different cutting edge microgeometries (distinct values of both the cutting edge segment on the flank face—S_α and the cutting edge segment on the rake face—S_γ) including symmetric ($S_\alpha = S_\gamma$) and asymmetric ($S_\alpha \neq S_\gamma$) edge preparations, the following conclusions can be drawn:

- Cutting edge preparation affects mainly the passive and feed forces (F_p and F_f, respectively), which increase with S_α and S_γ due to the more dominant ploughing effect caused by blunter tools (greater tool-workpiece contact length). As a consequence, F_p and F_f recorded for sharp tools (262 and 172 N, respectively) increased to 1064 and 455 N when tools with $S_\alpha = S_\gamma$ = 100 μm were used to turn AISI 4340 steel hardened to 50 HRC at a feed rate of 0.3 mm. High thrust forces can impair the machined surface quality; however, this damage can be avoided by applying reduced edge hones. As these force components did not affect the cutting forced drastically (maximum variation of 35 % throughout the test programme), variation of microgeometry did not change the specific energy and consequently, the chip temperature (maximum value of T = 669 °C when turning the specimen hardened to 50 HRC at a feed rate of 0.15 mm).
- In general, an increase in feed rate from 0.15 to 0.30 mm contributes to the reduction of thrust/cutting force ratio and specific energy, more notably when tools with larger S_α and S_γ values are used. In contrast, chip temperature was not substantially affected by the elevation of feed rate, probably owing to the fact that thicker chips aided to conduct the generated heat away from the cutting zone.
- The elevation of workpiece hardness from 40 HRC to 50 HRC led to higher passive and feed forces due to the increased shear strength of the work material, thus causing higher temperatures and a slight increase in the specific energy.
- With regard to the average surface roughness of the machined surface, values ranging from 3.3 to 5.7 μm were recorded after turning the specimens at a feed rate of 0.30 mm without a clear trend indicating the influence of cutting edge preparation. Due to edge chipping, irregular marks on the roughness profile were noticed when a sharp edge was employed. Marks on the valley of the profile were observed after turning with rounded edges, this phenomenon being possibly related to work material side flow.

Acknowledgments The authors are grateful to the Brazilian-German Collaborative Research Initiative on Manufacturing Technology (CAPES/DFG BRAGECRIM 029/14) supported by the German Research Foundation and CAPES Foundation, Ministry of Education of Brazil. Additional thanks go to Prof. Reginaldo T. Coelho from the University of São Paulo, Brazil, for his support concerning process forces measurements.

References

1. Benlahmidi S, Aouici H, Boutaghane F, Khellaf A, Fnides B, Yallese MA (2016) Design optimization of cutting parameters when turning hardened AISI H11 steel (50 HRC) with CBN7020 tools. Int J Adv Manuf Technol. doi:10.1007/s00170-016-9121-3
2. Tang L, Gao C, Huang J, Lin X, Zhang J (2014) Experimental investigation of the three-component forces in finish dry hard turning of hardened tool steel at different hardness levels. Int J Adv Manuf Technol 70:1721–1729
3. Yussefian NZ, Koshy P, Buchholz S, Klocke F (2010) Electro-erosion edge honing of cutting tools. CIRP Annals – Manuf Technol 59:215–218
4. Aurich JC, Zimmermann M, Leitz L (2011) The preparation of cutting edges using a marking laser. Prod Eng Res Devel 5:17–24
5. Fernández-Abia AI, Barreiro J, López de Lacalle LN, González-Madruga D (2014) Effect of mechanical pre-treatments in the behaviour of nanostructured PVD-coated tools in turning. Int J Adv Manuf Technol 73:1119–1132
6. Sharma V, Pandey PM (2016) Geometrical design optimization of hybrid textured self-lubricating cutting inserts for turning 4340 hardened steel. Int J Adv Manuf Technol. doi:10.1007/s00170-016-9163-6
7. Thiele JD, Melkote SN (1999) Effect of cutting edge geometry and workpiece hardness on surface generation in the finish hard turning of AISI 52100 steel. J Mater Process Technol 94:216–226
8. Meyer R, Köhler J, Denkena B (2012) Influence of the tool corner radius on the tool wear and process forces during hard turning. Int J Adv Manuf Technol 58:933–940
9. Chinchanikar S, Choudhury SK (2016) Cutting force modeling considering tool wear effect during turning of hardened AISI 4340 alloy steel using multi-layer TiCN/Al2O3/TiN-coated carbide tools. Int J Adv Manuf Technol 83:1749–1762
10. Özel T (2003) Modeling of hard part machining: effect of insert edge preparation in CBN cutting tools. J Mater Process Technol 141:284–293
11. Denkena B, Lucas A, Bassett E (2011) Effects of the cutting edge microgeometry on tool wear and its thermomechanical load. CIRP Annals – Manuf Technol 60:73–76
12. Kurt A, Şeker U (2005) The effect of chamfer angle of polycrystalline cubic boron nitride cutting tool on the cutting forces and the tool stresses in finishing hard turning of AISI 52100 steel. Mater Des 26:351–358
13. Chen L, El-Wardany TI, Nasr M, Elbestawi MA (2006) Effects of edge preparation and feed when turning hard turning a hot work die steel with polycrystalline cubic boron nitride tools. CIRP Annals - Manuf Technol 55:89–92
14. Davoudinejad A, Noordin MY (2014) Effect of cutting edge preparation on tool performance in hard-turning of DF-3 tool steel with ceramic tools. J Mater Process Technol 28:4727–4736
15. Khalili K, Safaei M (2009) FEM analysis of edge preparation for chamfered tools. Int J Mater Form 2:217–224
16. Denkena B, Köhler J, Mengesha MS (2012) Influence of the cutting edge rounding on the chip formation process: part 1. Investigation of material flow, process forces and cutting temperature. Prod Eng Res Devel 6:329–338
17. Denkena B, Biermann D (2014) Cutting edge geometries. CIRP Annals – Manuf Technol 63:631–653
18. Basset E, Köhler J, Denkena B (2012) On the honed cutting edge and its side effects during orthogonal turning operations of AISI 1045 with coated WC-Co inserts. CIRP J Manuf Sci Technol 5:108–126